© 2018. Published by The Company of Biologists Ltd | Journal of Cell Science (2018) 131, jcs206896. doi:10.1242/jcs.206896

RESEARCH ARTICLE

Calcium signaling mediates five types of cell morphological changes to form neural rosettes

Hana Hříbková[1], Marta Grabiec[1], Dobromila Klemová[2], Iva Slaninová[1] and Yuh-Man Sun[1,*]

ABSTRACT

Neural rosette formation is a critical morphogenetic process during neural development, whereby neural stem cells are enclosed in rosette niches to equipoise proliferation and differentiation. How neural rosettes form and provide a regulatory micro-environment remains to be elucidated. We employed the human embryonic stem cell-based neural rosette system to investigate the structural development and function of neural rosettes. Our study shows that neural rosette formation consists of five types of morphological change: intercalation, constriction, polarization, elongation and lumen formation. Ca^{2+} signaling plays a pivotal role in the five steps by regulating the actions of the cytoskeletal complexes, actin, myosin II and tubulin during intercalation, constriction and elongation. These, in turn, control the polarizing elements, ZO-1, PARD3 and β-catenin during polarization and lumen production for neural rosette formation. We further demonstrate that the dismantlement of neural rosettes, mediated by the destruction of cytoskeletal elements, promotes neurogenesis and astrogenesis prematurely, indicating that an intact rosette structure is essential for orderly neural development.

KEY WORDS: Embryonic stem cells, Neural stem cell niche, Neural rosette formation, Calcium, Neurogenesis, Adherens junctions, Cytoskeleton proteins

INTRODUCTION

Morphogenesis is a pivotal process during embryo development through which embryos shape their body, organize tissues and form organs. Morphogenesis occurs in all cell types in the body and occurs in many forms. Rosette organization is one such process occurring in various tissues and organs in a variety of organisms, which might reflect its functional significance or selective advantage. Rosette structures have been observed in *Drosophila* epithelial morphogenesis (Blankenship et al., 2006), zebrafish posterior lateral line primordium (Gompel et al., 2001) and Kupffer's vesicles (Oteiza et al., 2010), *Xenopus* kidney development (Lienkamp et al., 2012), the chick pre-streak blastoderm (Yanagawa et al., 2011), mouse pancreatic branching morphogenesis (Villasenor et al., 2010) and visceral endoderm development (Trichas et al., 2012), and vertebrate neural tube formation (Afonso and Henrique, 2006; Eom et al., 2011; Haigo et al., 2003; Nishimura and Takeichi, 2008; Harding et al., 2014).

[1]Department of Biology, Faculty of Medicine, Masaryk University, Brno 62500, Czech Republic. [2]Department of Histology and Embryology, Faculty of Medicine, Masaryk University, Brno 62500, Czech Republic.

*Author for correspondence (wadeley@med.muni.cz)

M.G., 0000-0003-3709-0866; Y.-M.S., 0000-0002-8863-4280

Received 30 May 2017; Accepted 18 December 2017

Rosette structures also take part in morphogenesis during neural development. The central nervous system (CNS) develops initially from a monolayer of neuroepithelial (NE) cells, which then roll up to form the neural tube. Within the neural tube, neural stem cells (NSCs) organize to form rosette structures (called neural rosettes), which have been reported *in vivo* and *in vitro* (Banda et al., 2015; Colleoni et al., 2010; Curchoe et al., 2012; Elkabetz et al., 2008; Grabiec et al., 2016; Harding et al., 2014; Mirzadeh et al., 2008; Paşca et al., 2015). Pluripotent stem cell (PSC)-based *in vitro* systems recapitulate embryonic brain development in many aspects; for example, the temporal appearance and spatial locations of neural cells, and the microenvironment regulating NSCs (Falk et al., 2016; Lancaster et al., 2013; Shi et al., 2012; Ziv et al., 2015). NSCs undergo orderly proliferation and differentiation under the control of NSC niches residing within neural rosettes (Cheng et al., 2003; Gaiano and Fishell, 2002; Gilbert, 2010), suggesting the importance of neural rosette structures.

Pluripotent stem cell (PSC)-based neural developmental modeling provides a good system for exploring neural rosette formation. Along with others, we have shown that during the course of neural differentiation from PSCs, NSCs begin to appear about 4 days after the start of differentiation, followed by neural rosette formation, during which mature neural rosettes can be seen from day 9 (Zhang et al., 2001; Perrier et al., 2004; Elkabetz et al., 2008; Boroviak and Rashbass, 2011; Curchoe et al., 2012; Shi et al., 2012; Paşca et al., 2015; Grabiec et al., 2016). Previous studies revealing the characteristics of neural rosettes include: apical–basal polarity (Elkabetz et al., 2008; Boroviak and Rashbass, 2011; Abranches et al., 2009; Ziv et al., 2015; Grabiec et al., 2016), apical localisation of ZO-1, N-cadherin, β-catenin, Par3/aPKC. Numb, Crumbs, Cdc42, Pals1, PatJ, FGF2, FGF receptors, prominin, actin and Notch1 (Elkabetz et al., 2008; Boroviak and Rashbass, 2011; Abranches et al., 2009; Ziv et al., 2015; Grabiec et al., 2016), and interkinetic nuclear migration (Wilson and Stice, 2006; Abranches et al., 2009). However, the molecular and cellular mechanisms underlying morphogenetic movements during rosette formation remain an open question in developmental biology. This study was undertaken to determine how neural rosettes form, which factors are involved, and their potential roles in neural fate decisions using a human PSC-based system.

RESULTS

Neural rosette formation comprises five steps of cell morphological changes

To elucidate the function of neural rosettes, we first established the structure of the cell assembly during neural rosette formation by investigating the localization of adherens junctions and cytoskeletal proteins. To this end, we employed a human embryonic stem cell (hESC)-based neural developmental modeling system, in which neural induction occurred after 4 days of differentiation (D4), neural rosettes started to assemble from D5, and formed at around D9 (Grabiec et al., 2016).

Journal of Cell Science (2018) 131, jcs206896. doi:10.1242/jcs.206896

Our data showed that β-catenin appeared in adherens junctions after neural induction (D5) and gradually polarized and formed a ring structure in the apical region of neural rosettes (D8–D9) (Fig. 1A). ZO-1 initially localized at tight junctions during early development (D5) (Movie 1), gradually dissolved (around D7–D8) when neural rosettes formed (Movie 2), and then became polarized and colocalized with β-catenin in the apical region of neural rosettes (Fig. 1A,B). The localization of PARD3 was similar to that of ZO-1; however, unlike ZO-1, PARD3 did not disperse before polarizing to form a ring structure (Fig. 1A,B). Tubulin also showed similar polarization during neural rosette formation, but without forming a ring structure (Fig. 1A,B). We further used these four proteins to investigate cell movement and morphological changes during neural rosette formation. We found that cells underwent five distinctive changes in morphology and movement to form neural rosettes, which included cell intercalation (two or more rows of cells move between one another), constriction (cells contract or shrink), polarization, elongation and lumen formation (Fig. 2). Among these cell movements, constant interactions were observed that culminated in a mature neural rosette formation, which was characterized by lumen formation in the apical region of neural rosettes (Fig. 2).

The electron microscopic view of neural rosettes

To understand the possible functions of neural rosettes, we further analyzed the structure of neural rosettes using electron microscopy (Fig. 3). This revealed that elongated neural epithelial cells (or NSCs) connected to adjacent cells with adhesions and tight junctions. NSCs were 'chained' together with actin bundles that were wrapped around the neck of the apical end-feet of neural rosettes. This resembled a purse string that tightened and constricted the apical ends of rosettes (Fig. 3C,F), so that they radiated out around the lumen (Fig. 3B,D). This phenomenon could also be seen under immunocytochemical staining, which showed that a ring structure formed around the lumen (Fig. 3A; Fig. 1A,B). We observed that the lumen structure was dynamic and constantly being restructured and reshaped (Movie 3). Interkinetic nuclear migration (INM), which has been documented in previous studies (Wilson and Stice, 2006; Abranches et al., 2009), was also observed in NSCs in neural rosettes. During INM, the nuclei of NSCs migrated between the apical and basal regions in coordination with the cell cycle and underwent mitosis at the apical region (Fig. 3D,E). This peculiar behavior of NSCs can be explained by the structural arrangement of neural rosettes (Fig. 3F). In the apical region, we found that each NSC possessed a single primary cilium, which connected to the mother centriole at one end, with the other end protruding from the apical end-feet into the lumen, whereby the primary cilium received cues from the lumen that hosted many regulatory elements. It has been well documented that during cell mitosis, centrosomes interact with the chromosomes to build the mitotic spindle for chromosome segregation (Bornens and Azimzadeh, 2008). This might be one of

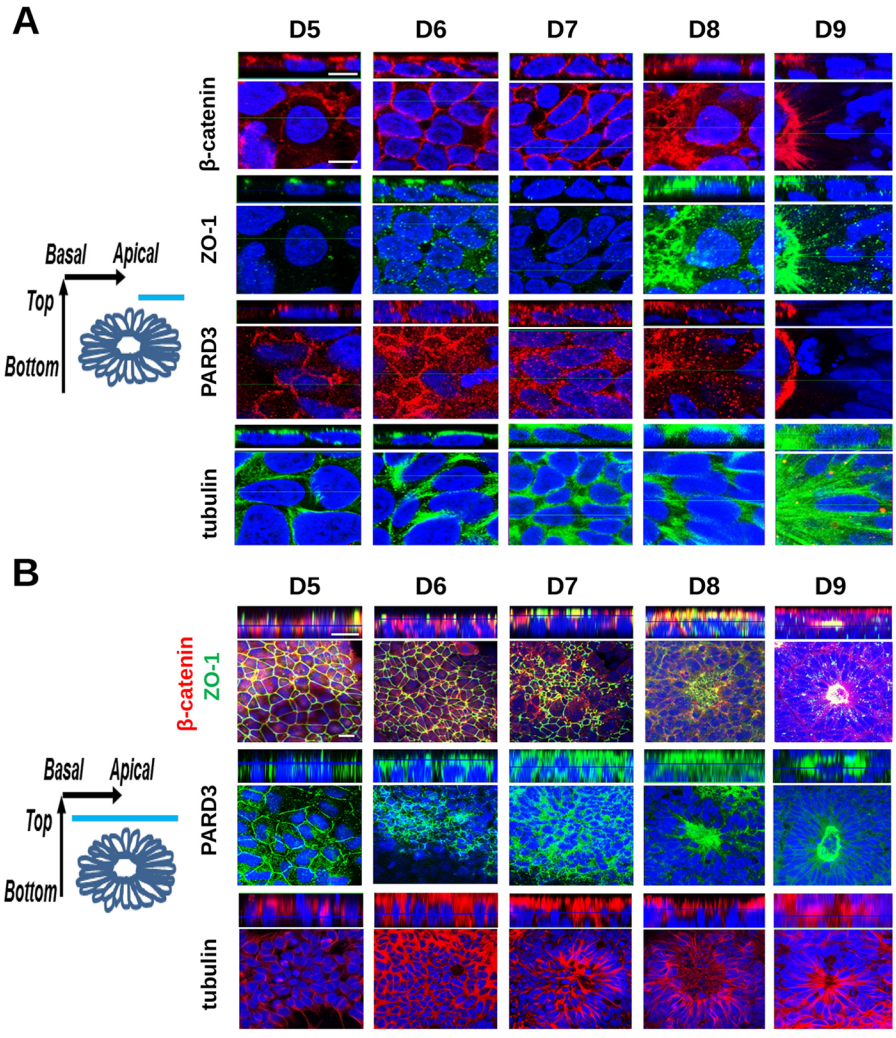

Fig. 1. Stages of neural rosette formation. Human embryonic stem cells were driven towards neural differentiation and samples were collected from D5 to D9. (A) Topographic views of the different stages of rosette formation at the angle indicated by light blue line in the diagram on the left, which depicts 3D orientation of neural rosettes. The localization of β-catenin, ZO-1, PARD3 and tubulin during rosette formation is shown in one-plane images (bottom) with *Z*-stack images shown above. Scale bars: 5 µm. (B) Topographic views of the top of neural rosettes during their formation as indicated by light blue line in the diagram. Localization of β-catenin, ZO-1, PARD3 and tubulin during rosette formation is shown in one-plane images (bottom) with Z-stack images above. Scale bars: 20 µm. Nuclei are stained blue with DAPI. Experiments were repeated three times.

Journal of Cell Science (2018) 131, jcs206896. doi:10.1242/jcs.206896

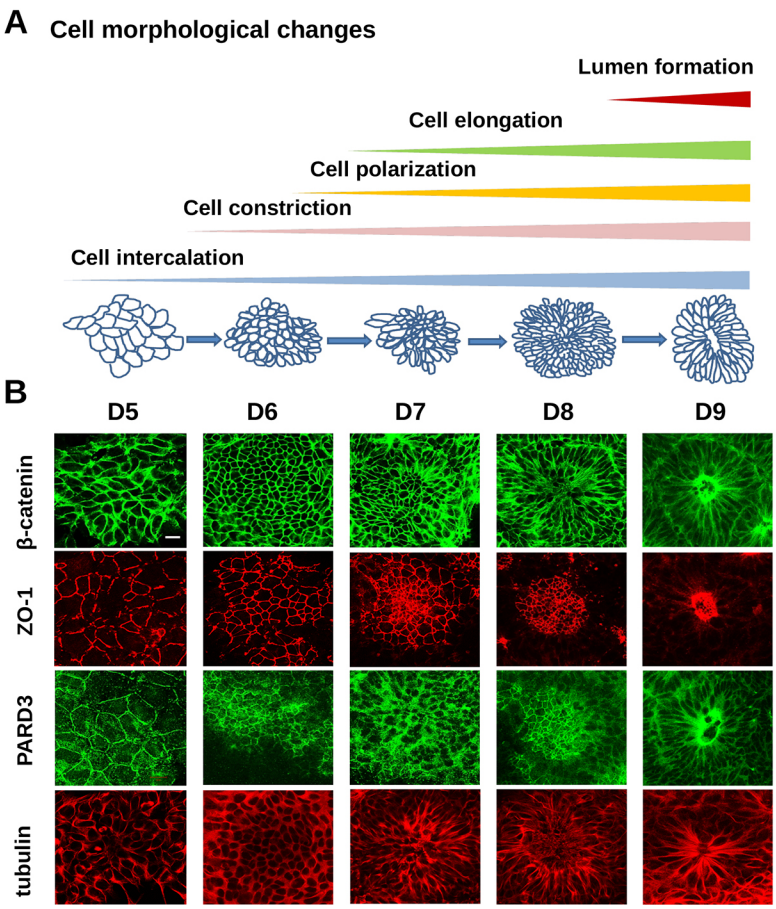

Fig. 2. Cell morphological changes during rosette formation. (A) The morphogenesis of neural rosettes is classified into five steps based on cell morphological changes during neural rosette formation judged by adherens and cytoskeletal proteins shown in B, which are presented in schematic drawings. The five types of cell morphological changes, from early to late stages of neural rosette formation (D5–D9), included intercalation, constriction, polarization, elongation and lumen formation. (B) The localization of β-catenin, ZO-1, PARD3 and tubulin during neural rosette formation as depicted in A. Scale bar: 20 µm. Experiments were repeated three times.

the reasons that cell mitosis occurred at the apical region of neural rosettes (Fig. 3E).

Lumens are formed via apoptosis and are crucial for neurogenesis

While we were examining rosette structures using electron microscopy, we noticed that there were many apoptotic-like cells in the area of newly formed lumens (Fig. 4A). We postulated that lumen formation might result from cavitation due to cell apoptosis. To test our theory, we examined neural rosettes during the initiation of lumen formation using immunocytochemical analysis with cleaved caspase-3 antibody, which is a marker of apoptosis. We found that cells in many lumens stained positively with the cleaved caspase-3 antibody (Fig. 4A), suggesting that cells underwent apoptosis, which corroborated our observations with electron microscopy. We further tested whether apoptotic inhibitors could prevent lumen formation. We examined the process of lumen formation in the presence of various doses of the pan-caspase inhibitor z-VAD-FMK (z-VAD) (10 µM, 20 µM and 40 µM). Our results showed that 40 µM z-VAD prevented cell apoptosis and also abolished lumen formation (Fig. 4B). This supported our theory that cell apoptosis is involved in lumen formation. Based on the idea that lumens are one of the crucial features in neural rosettes, we were interested in establishing what role lumens played during neural development. We conducted an experiment to evaluate neurogenesis in neural rosettes that were rendered devoid of lumens under treatment with 40 µM z-VAD. Interestingly, we found that the z-VAD treatment retarded neurogenesis relative to the control group, suggesting that lumens might play a regulatory role in ensuring the orderly production of neurons (Fig. 4C). To further establish the potential role of lumens in neural rosettes, we investigated the effect of manually destroyed lumens. Surprisingly, we found that the dismantlement of lumens did not lead to reassembly of the original neural rosettes, instead it resulted in more rosettes (data not shown), suggesting how dynamic and resilient neural rosettes are and how crucial the lumen is in the maintenance of rosette structures. Collectively, our finding shows that lumens take part in constructing neural rosettes and neural differentiation.

Neural rosette disarray during dysregulation of Ca^{2+} signaling

As Ca^{2+} signaling has been shown to play a crucial role in morphogenesis (Brennan et al., 2005; Wallingford et al., 2001; Webb and Miller, 2003), we wondered whether Ca^{2+} was also involved in neural rosette formation and maintenance. We tested the effect of Ca^{2+} by examining the response of neural rosettes in Ca^{2+} free HBSS buffer using immunocytochemical analysis and time-lapse imaging. Our results showed that neural rosettes completely dismantled within 30 min of being placed in HBSS buffer and the surviving cells were enlarged after 4 h of treatment, accompanied by translocation of adherens and tight junction proteins, β-catenin and ZO-1 (Fig. 5A). During the early stage of the 4 h HBSS treatment, the two proteins mainly co-polarized at the top of cells after about 30 min and gradually ZO-1 localized to adherens junctions after about 1 h of treatment, which was distinct from β-catenin localization (Fig. 5A). Interestingly, both proteins formed aggregates on the side or the top of nuclei after about 2 h of treatment and some of the β-catenin partitioned into nuclei after 4 h of treatment, while ZO-1 remained at adherens junctions (Fig. 5A).

Journal of Cell Science (2018) 131, jcs206896. doi:10.1242/jcs.206896

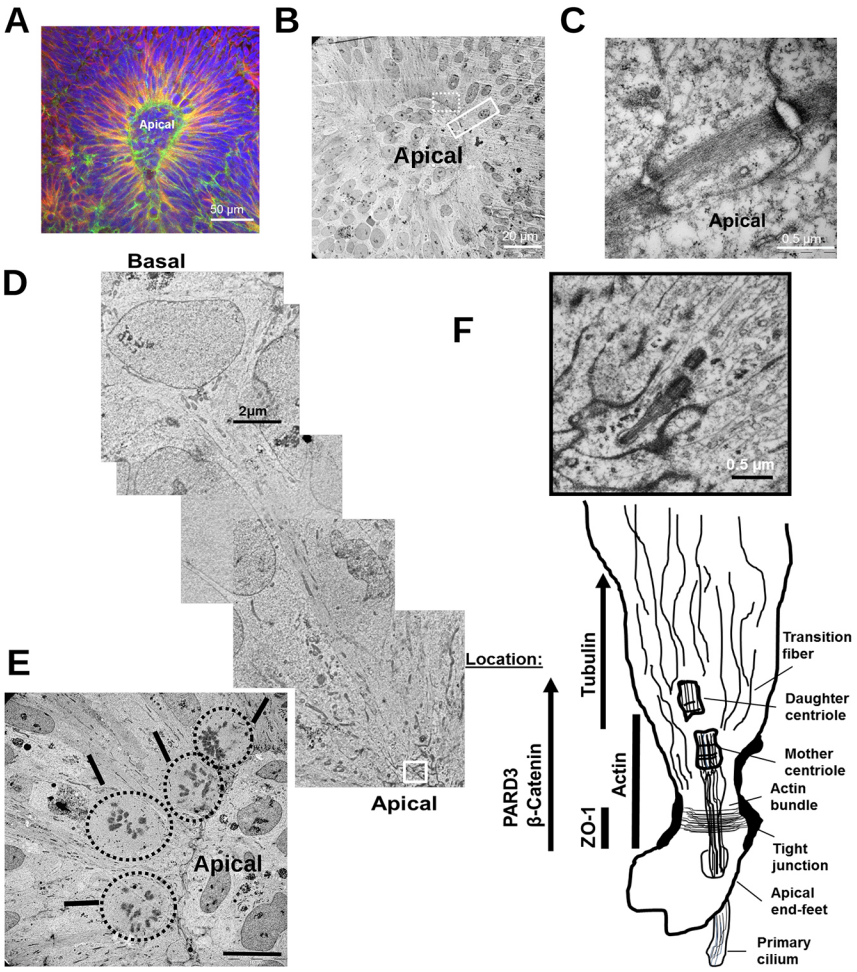

Fig. 3. Electron microscopic images of neural rosettes. (A) A representative mature neural rosette stained with actin (green) and tubulin (red) exhibits a lumen located in the apical region. Nuclei are stained blue with DAPI. Scale bar: 50 µm. (B) Electron microscopic image of a neural rosette with a lumen in the center (the apical region). The boxed regions with dashed and solid lines are enlarged and presented in C and D, respectively. Scale bar: 20 µm. (C) An enlarged apical region of a neural rosette, where the apical end-feet of neural stem cells are arrayed neatly along the lumen. Actin bundles tightly wrapped around the end-feet with adhesions and tight junctions are visible, which form a ring structure that was also seen in A and Fig. 1. Scale bar: 0.5 µm. (D) A montage of images depicting an elongated neural stem cell extending from the basal region to the apical region of neural rosettes. The primary cilium, located in the apical region, is marked with a box, enlarged, and presented in F. Scale bar: 2 µm. (E) Mitotic cells (circled) in the apical region of neural rosettes. Scale bar: 10 µm. (F) Location of the primary cilium in the apical end-feet of neural stem cells shows that one end connects to the mother centriole, which is accompanied by the daughter centriole, while its other end protrudes into the lumen (depicted in the bottom panel). Scale bar: 0.5 µm. The bottom panel is a schematic diagram showing the essential components in the apical region of neural stem cells and the localization of ZO-1, PARD3, β-catenin and tubulin; diagram is based on data derived from electron microscopic imaging and immunocytochemical analysis.

Although neural rosettes were destroyed after 30 min in HBSS, the effect was reversible, which can be seen in our confocal time-lapse imaging (Movie 4). However, restructured neural rosettes looked different from the original forms, suggesting that cells are dynamic in reshaping themselves.

We next investigated whether Ca^{2+} from internal stores plays a role in neural rosette formation and maintenance. We treated cells during rosette formation with an IP3 receptor blocker, 2-APB, which decreased $[Ca^{2+}]_i$ levels by blocking Ca^{2+} release from the internal stores via IP3 receptors. We found that not only did neural stem cells fail to generate neural rosettes, but the cells also enlarged enormously (Fig. 5B). This might have resulted from the impairment in cell constriction, polarization and elongation after 2-APB treatment, possibly by disrupting adherens and tight junction proteins. It was apparent that the effect of 2-APB on the distribution of β-catenin and ZO-1 exhibited similar patterns to those observed during HBSS treatment, in which ZO-1 was translocated to adherens junctions while β-catenin moved to the cytosol and nucleus (Fig. 5B). To investigate the effect of 2-APB on neural rosette maintenance, we used time-lapse imaging to record the impact of 2-APB on neural rosettes. Our results showed that 2-APB treatment caused the disintegration of neural rosettes at a more gradual pace than HBSS. It is worth noting that unlike HBSS treatment, the dismantled neural rosettes did not re-establish rosette structures after removing 2-APB solution (Movie 5). Our findings also showed that PARD3, a polarity protein, was depolarized from the apical region and relocated to the cell membrane, cytosol and nucleus after 2-APB treatment, similarly to the cytosolic relocation of actin and tubulin (Fig. 5C). These findings suggest that intracellular Ca^{2+} plays a role in polarization.

We also examined the effect of thapsigargin, an inhibitor of the sarco-endoplasmic reticulum calcium ATPase (SERCA), on neural rosettes, which yielded no results because of the toxicity of the drug (not shown). We further characterized the impact of extracellular Ca^{2+} on neural rosette formation and maintenance using the dihydropyridine L-type voltage-sensitive calcium-channel blocker Nifedipine. We found that 20 µM Nifedipine exerted very little impact on rosette formation and maintenance (Fig. 5B), which might have been compensated for by other functional Ca^{2+} channels. Our results suggest that Ca^{2+}, especially from internal stores, plays a crucial role in rosette formation and maintenance.

Cytoskeletal elements play crucial roles in neural rosette formation

After finding, as shown above, that actin, myosin II and tubulin were important structural elements of neural rosettes, we next set out to test the roles of those proteins in neural rosette formation using biochemical approaches. We found that treatment with cytochalasin D (CytoD), which blocks polymerization and the elongation of actin, resulted in puncta staining of actin and disrupted neural rosette formation by abolishing apical polarization of β-catenin, ZO-1, PARD3 and tubulin, which led to the proteins remaining in the cytosol (Fig. 6A,B). Treatment with the myosin II inhibitor blebbistatin caused more drastic changes in cell phenotypes, including dismantlement of neural rosettes, and production of giant cells with multiple nuclei, possibly due to cell nondisjunction

Journal of Cell Science (2018) 131, jcs206896. doi:10.1242/jcs.206896

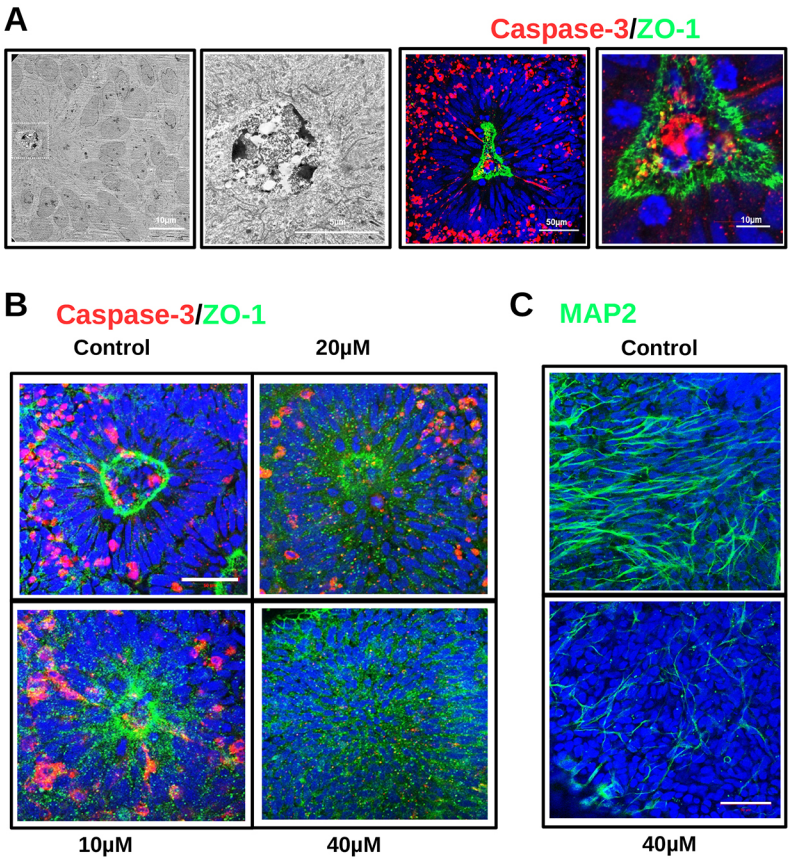

Fig. 4. The formation and function of lumens in neural rosettes. (A) The involvement of apoptosis in lumen formation during neural rosette maturity is shown by electron microscopy (first two images) and immunocytochemical analysis. Cells were stained with antibodies against cleaved caspase-3 (red) and ZO-1 (green), in which positively stained cells represent apoptotic cells and the lumen, respectively. Scale bars: 10, 5, 50 and 10 μm (from left to right). (B) Inhibition of apoptosis using z-VAD during neural rosette formation prevented lumen formation. Neural stem cells were treated with various doses of z-VAD (indicated) from D6 and were fixed at D9. They were immunostained with antibodies against cleaved caspase-3 (red) and ZO-1 (green). (C) The lumen-less structure impaired neurogenesis. Cells were continuously treated with 40 μM z-VAD from D6 to D20, then fixed and stained for the neuronal marker MAP2. Scale bar: 20 μm (B and C). Nuclei are stained blue with DAPI. Experiments were repeated twice.

associated with a nonfunctional actomyosin ring and the impairment of cytokinesis. Moreover, ZO-1, β-catenin, PARD3, actin and tubulin were relocated to the cytosol, cell membrane and even to the nucleus. Interestingly, treatment with ML-7, which is a selective inhibitor of myosin light chain kinase, caused less damage to neural rosettes. We observed that some neural rosettes disappeared, but some remained (Fig. 6A,B). Nocodazole, an inhibitor of microtubules polymerization, abolished cell elongation, caused cell expansion, reduced cell contact, and relocated β-catenin and PARD3 to the cytosol and nucleus, and ZO-1 and actin to adherens junctions, which led to a failure of neural rosette formation (Fig. 6A,B).

We have shown that polarization is a crucial step during neural rosette formation (Figs 1 and 2). We wondered what effect polarization would have on neural rosette formation. To address this question, we investigated the impact of ZO-1, an important polarizing element, on the polarization of β-catenin, PARD3 and tubulin during neural rosette formation. To this end, we generated ZO-1 knockdown human ESCs and drove their differentiation towards a neural lineage. Samples were then examined during the period of rosette formation. We found that knockdown of ZO-1 impeded the apical polarization of β-catenin, PARD3 and tubulin, which caused neural rosette formation to cease (Fig. 7). Our results suggested that ZO-1 takes part in the apical polarization of those elements and might result in the impairment of lumen formation, which was suggested by the formation of ring-like structures.

Neural rosettes govern neural fate decisions

We next established the role of rosette structures in neural fate decisions using biochemical approaches. We examined the effect of inhibiting crucial elements of neural rosettes on neurogenesis and astrogenesis using various inhibitors, including Nifedipine and 2-APB for $[Ca^{2+}]_i$ levels, CytoD for actin, blebbistatin for myosin II and ML-7 for myosin light chain kinase. Neural rosettes derived from human ESCs were harvested after D8 and were continuously treated with the aforementioned inhibitors for 3 days after the cells had adhered to plates. Cell samples were collected and analyzed for the production of neurons and astrocytes after differentiation for 14, 30, 40, 50 and 60 days (Fig. 8). We found that most inhibitors did not affect cell survival. The exception was CytoD treatment (2 h every 3 days) for 60 days; this resulted in a 60% reduction in cell numbers, despite the fact that there was no significant cell loss after D50. Treatment with CytoD, blebbistatin, ML-7 and 2-APB resulted in a dismantling of rosette structures, while there were many neural rosettes present in the control group. Intriguingly, accompanying the destruction of neural rosettes, we also observed that neurogenesis occurred early, after around 14 days of differentiation, when treated with the four inhibitors, which produced 5–20% $MAP2^+$ neurons compared with the control group, which generated few, if any positive cells (Fig. 8A). This advanced neurogenesis progressed to 30 days, after which all inhibitor treatments generated more than 55% $MAP2^+$ neurons compared with just under 40% positive neurons in control cells. However, this early neurogenesis, under the influence of the inhibitors, disappeared after D40, i.e. neuronal production in control cells had caught up at D40, D50 and D60 (Fig. 8A). Our results suggested that Ca^{2+}, actin and myosin play pivotal roles in maintaining neural rosette structures and in generation of neurons.

In the next step, we tested the impact of these inhibitors on astrogenesis. Our results showed that the treatment with CytoD, ML-7 and 2-APB advanced astrogenesis, in which we observed 1–2% $GFAP^+$ astrocytes after D50, while very few, if any positive

Journal of Cell Science (2018) 131, jcs206896. doi:10.1242/jcs.206896

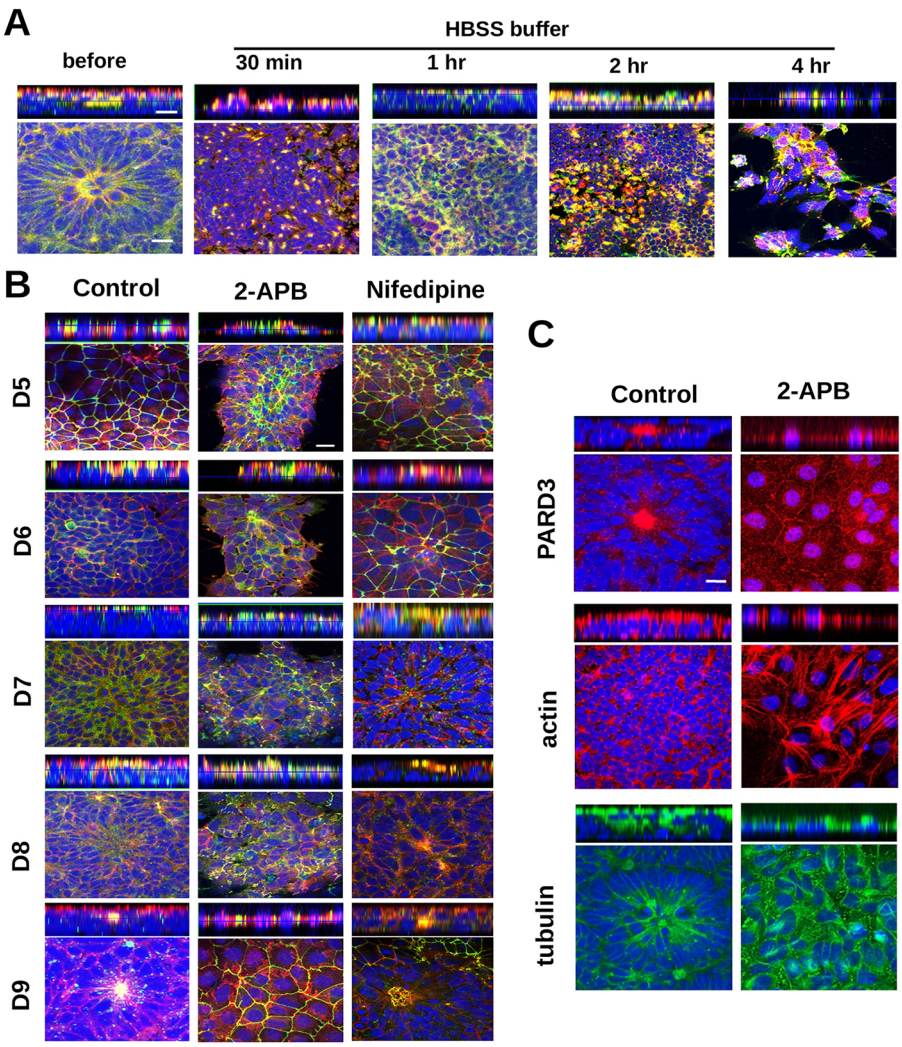

Fig. 5. The effect of Ca^{2+} on neural rosette formation and maintenance. (A) Neural rosettes disassembled in a Ca^{2+}-free environment (in HBSS buffer). Human ESC-derived neural rosettes were treated with Ca^{2+}-free HBSS buffer for various time periods (indicated) and fixed immediately afterward. The samples were immunostained with antibodies against β-catenin (red) and ZO-1 (green). The localization of β-catenin and ZO-1 are shown in one-plane images (bottom) with *Z*-stack images above. (B) Ca^{2+} from internal stores played a crucial role in neural rosette formation. Human ESCs were driven towards neural differentiation, during which neural rosettes generally formed around D9. Cells were treated with an IP3 receptor blocker, 50 µM 2-aminoethoxydiphenyl borate (2-APB) or a L-type voltage-sensitive calcium-channel blocker nifedipine (20 µM), from D4 to D9. Cells were fixed on various days (indicated) and stained for β-catenin (red) and ZO-1 (green). (C) The effect of 2-APB on the localization of cytoskeletal proteins and PARD3 in neural rosettes at D9. Cells were treated with 2-APB during neural rosette formation (from D4 to D9) and fixed at D9. Nuclei are stained blue with DAPI. Scale bars: 20 µm. Experiments were repeated three times.

cells were seen in the control. As differentiation proceeded, three of the inhibitors produced over 5% astrocytes, with CytoD treatment producing 3%; all values were higher than that in the controls (<1%) (Fig. 8B). Collectively, our results suggested that NSCs residing in rosette organizations are providing essential niches to ensure orderly neural fate decisions. If the structure of neural rosettes is disrupted, e.g. by inhibitors, alteration of NSC niches ensues, which in turn leads to changes in the temporal appearance of neural cells.

It is worth noting that an interesting phenomenon was observed during treatment with ML-7: neurons were generated with normal-sized cell bodies, but very short processes, through to D60 (Fig. 8A). Surprisingly, the phenomenon was not observed in the derived interlaminar astrocytes, which showed normal process lengths (Fig. 8B). Our results suggest that the effect of ML-7 on process growth is specific to neurons, implying that the mechanisms underlying elongation of neuronal processes is different to those in astrocytes.

DISCUSSION

A range of morphogenetic cell movements are required for the development of vertebrate embryos and the generation of tissues and organs. Ca^{2+} signaling has been demonstrated to play an important role in coordinating complex cell movements. Wallingford et al. (2001) reported that dramatic intercellular waves of Ca^{2+} mobilization occurred in cells undergoing convergent extension in explants of gastrulating *Xenopus* embryos, in which cells intercalate, constrict and elongate the embryonic axis. Furthermore, depletion of Ca^{2+} from the endoplasmic reticulum abolished the process of convergent extension. These propagating Ca^{2+} waves have been considered to be a common feature of vertebrate convergent extension and the formation of the paraxial mesoderm in zebrafish embryos (Brennan et al., 2005; Webb and Miller, 2003), as well as in chicks and mice (Webb and Miller, 2006). Our findings echo these studies by showing that inhibition of Ca^{2+} signaling abolishes constrictions in neural rosettes with a lesser effect on cell intercalations. Our study further shows that impediment of cell constrictions results in the generation of enlarged cells, which are also accompanied by aberrant localization of neural rosette structural elements (i.e. actin, tubulin, ZO-1, PARD3 and β-catenin), which leads to abrogation of the downstream steps of neural rosette formation, including apical constriction, polarization, elongation and lumen formation. Our data suggest that Ca^{2+} is a key factor involved in initiating neural rosette formation.

We and others have showed that the neural differentiation of pluripotent stem cells (PSCs) recapitulate brain developmental processes *in vivo* (Wilson and Stice, 2006; Elkabetz et al., 2008; Sun et al., 2008; Curchoe et al., 2012; Shi et al., 2012; Paşca et al., 2015; Grabiec et al., 2016). PSCs undergo morphogenetic events characterized by the formation of radially organized columnar

Journal of Cell Science (2018) 131, jcs206896. doi:10.1242/jcs.206896

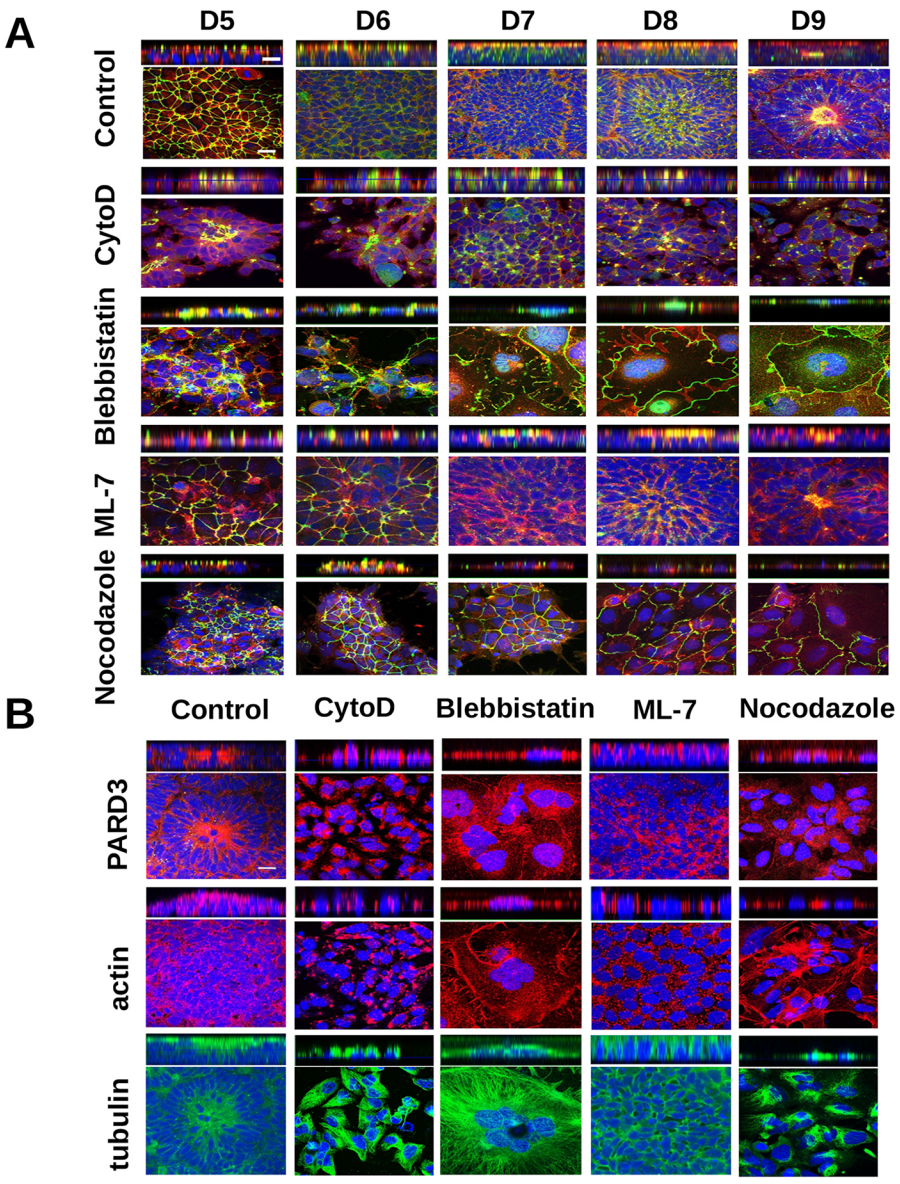

Fig. 6. Multiple factors are involved in neural rosette formation. A range of inhibitors were used to explore the roles of actin (cytochalasin D, CytoD), myosin II (Blebbistatin), myosin light chain kinase (ML-7) and tubulin (nocodazole) during neural rosette formation. Human ESCs were plated out and differentiated towards neural rosette formation, during which cells were treated with individual inhibitors continuously from D4 to D9 and fixed on specific days (indicated). (A) Cells were stained to detect ZO-1 (green), β-catenin (red). (B) Cells were fixed at D9 and stained with antibodies against PARD3 (red), actin (red) and tubulin (green). The representative images are shown as one-plane images (bottom panel) with *Z*-stack images above. Nuclei are stained blue with DAPI. Scale bars: 20 µm. Experiments were repeated twice.

epithelial cells termed 'neural rosettes' (Zhang et al., 2001; Perrier et al., 2004). PSC-derived neural rosettes adopt polarized neuroepithelial structures with an anterior CNS fate (Elkabetz et al., 2008; Boroviak and Rashbass, 2011), with the tight junction protein ZO-1 and the adherens junction protein N-cad colocalizing in the apical region of neural rosettes. This is in line with our finding that ZO-1 colocalizes with another adherens junction protein, β-catenin, in the apical region of neural rosettes. However, our study goes further and demonstrates that the dynamic relocation of ZO-1 and β-catenin towards the apical region during neural rosette formation occurs between D5 and D9, and their movements are regulated by a variety of factors (see below). Moreover, our study also elucidates the effects of Ca^{2+} signaling, the inhibition of cytoskeletal elements (actin, myosin II and tubulin) and dysregulation of ZO-1 on neural rosette formation and maintenance.

The transformation of epithelial cells from a non-polarized state to a polarized phenotype is characterized by a reorganization of the plasma membrane into specialized domains and by the formation of apical and basolateral poles separated by junctional complexes (Collado-Hilly et al., 2010). Our electron microscopic analysis of neural rosettes shows that neural epithelial cells are neatly arrayed with adherens and tight junction complexes in the apical region and lead to apical constriction and polarization, possibly via actomyosin networks that tighten apical regions in a 'purse-string' fashion. Previous studies have shown that dysregulation of Notch signaling impairs apical polarity (Main et al., 2013) and Crumbs 2 is an apical polarity determinant (Boroviak and Rashbass, 2011).

In our study, we observed that neural rosettes were dismantled and cells were floating in Ca^{2+}-free HBSS, suggesting that Ca^{2+} is needed for cell adhesion, which is in line with a previous study showing that Ca^{2+}-free medium rapidly perturbs cell–cell contacts and causes a loss of adherens junctions, which leads to dramatically perturbed cell polarity (Dupin et al., 2009). We also found that apical constriction, polarization and elongation in neural rosettes are abolished in Ca^{2+}-free HBSS, suggesting that Ca^{2+} regulates the actions of cytoskeletal complexes (actin and tubulin) and polarizing elements (ZO-1, PARD3 and β-catenin) in maintaining neural rosettes. This is also echoed by the finding in MDCK cells that Ca^{2+}

Journal of Cell Science (2018) 131, jcs206896. doi:10.1242/jcs.206896

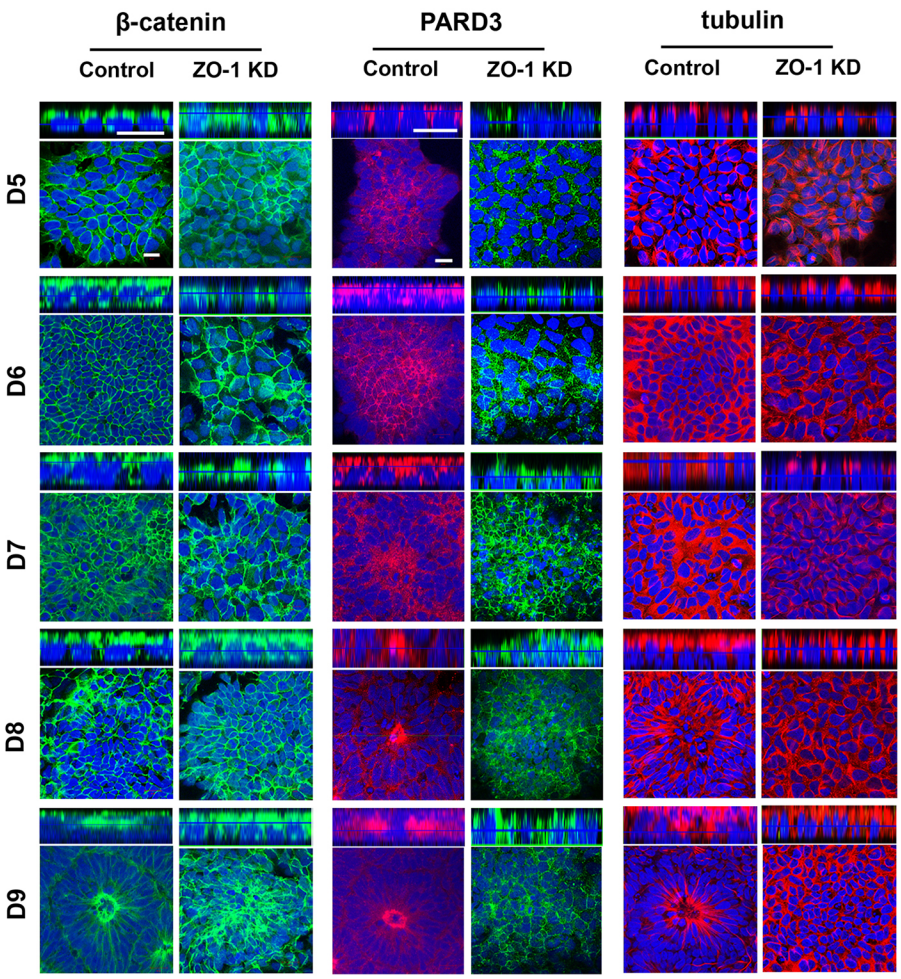

Fig. 7. Effects of knockdown of ZO-1 on β-catenin, PARD3 and tubulin localization during rosette formation. ZO-1 knockdown (ZO-1 KD) human ESCs were generated and differentiated towards a neural lineage. Samples were examined during rosette formation on days indicated. ZO-1 KD impeded apical polarization of β-catenin, PARD3 and tubulin, which ended neural rosette formation. Nuclei are stained blue with DAPI. Scale bars: 20 µm.

deprivation disrupted cell polarity, which restored by addition of Ca^{2+} (Colosetti et al., 2003). The pivotal role of Ca^{2+} in cell polarization has been shown in MDCK cells (Colosetti et al., 2003), exocrine acinar cells (Petersen and Tepikin, 2008), plant zygotes and tube cells (Bothwell et al., 2008; Hable and Hart, 2010; Himschoot et al., 2015), *Xenopus* gastrulation (Shindo et al., 2010) and human bone osteosarcoma cells (Huang et al., 2015). Moreover, we further found that the displacement of actin, tubulin, ZO-1, PARD3 and β-catenin resulted from 2-APB-mediated inhibition of Ca^{2+} signaling. We hypothesized that dysregulated Ca^{2+}-mediated dysfunction of actin and tubulin prevented apical constriction and elongation in neural rosettes, which in turn resulted in the aberrant localization of ZO-1, PARD3 and β-catenin, thus impeding cell polarization and lumen formation. Our theory was substantiated by our finding that the mislocalization of actin, tubulin, ZO-1, PARD3 and β-catenin in the presence of Ca^{2+} inhibition was similar to that caused by the inhibition of actin and tubulin, suggesting that Ca^{2+} is an initiator of a hierarchical chain reaction of neural rosette formation.

The important regulatory role of Ca^{2+} in the actions of actin, myosin and tubulin in neural rosettes mirrors previous findings that Ca^{2+} controls the dynamics of actin via protein kinase C and calmodulin-dependent kinases (Hoffman et al., 2013; Larsson, 2006), the formation of actin bundles through Rho GTPase signaling (Evans and Falke, 2007), and polymerization of actin via the F-actin-severing protein cofilin (Huang et al., 2011). Tsai and Meyer (2012) showed that local pulses of Ca^{2+} at junctions between lamellipodia and lamella activated myosin light chain kinase, which subsequently phosphorylated myosin light chain and triggered myosin contraction. The role of Ca^{2+} in regulating the function of cytoskeletal components in neural rosettes might extend to cell polarization. It has been shown that cytoskeletal elements are actively involved in the function, maintenance and restoration of tight junctions, which play an important role in the apical configuration of epithelial sheets (Glotfelty et al., 2014; Shen and Turner, 2005). Our results show that the inhibition of Ca^{2+} signaling and cytoskeletal elements exert similar characteristic effects on depolarizing molecules, which includes translocation of ZO-1 to adherens junctions, PARD3 and β-catenin to cytosol and nuclei, and cell depolarization. Our findings agree with a previous study in which global cell polarization, mediated by the actin–microtubule (MT) crosstalk at adhesion domains, was found to be regulated by Ca^{2+} signaling (Sackmann, 2015).

Additionally, our results show that inhibiting a $[Ca^{2+}]_i$ regulator, i.e. IP3 receptors, by treating cells with 2-APB, prevents neural rosette formation and polarization of β-catenin and ZO-1, suggesting that IP3 receptors play a crucial role in rosette formation possibly via cell polarization. Our finding is in line with previous observations showing that the role of Ca^{2+} in cell polarization is coincident with the polarization of IP3 receptor distribution (Collado-Hilly et al., 2010; Colosetti et al., 2003; Cruttwell et al., 2005). IP3 receptors are evenly distributed in the cytoplasmic ER in non-polarized cells, but are mostly distributed at the apex of the lateral plasma membrane along with the markers of

Journal of Cell Science (2018) 131, jcs206896. doi:10.1242/jcs.206896

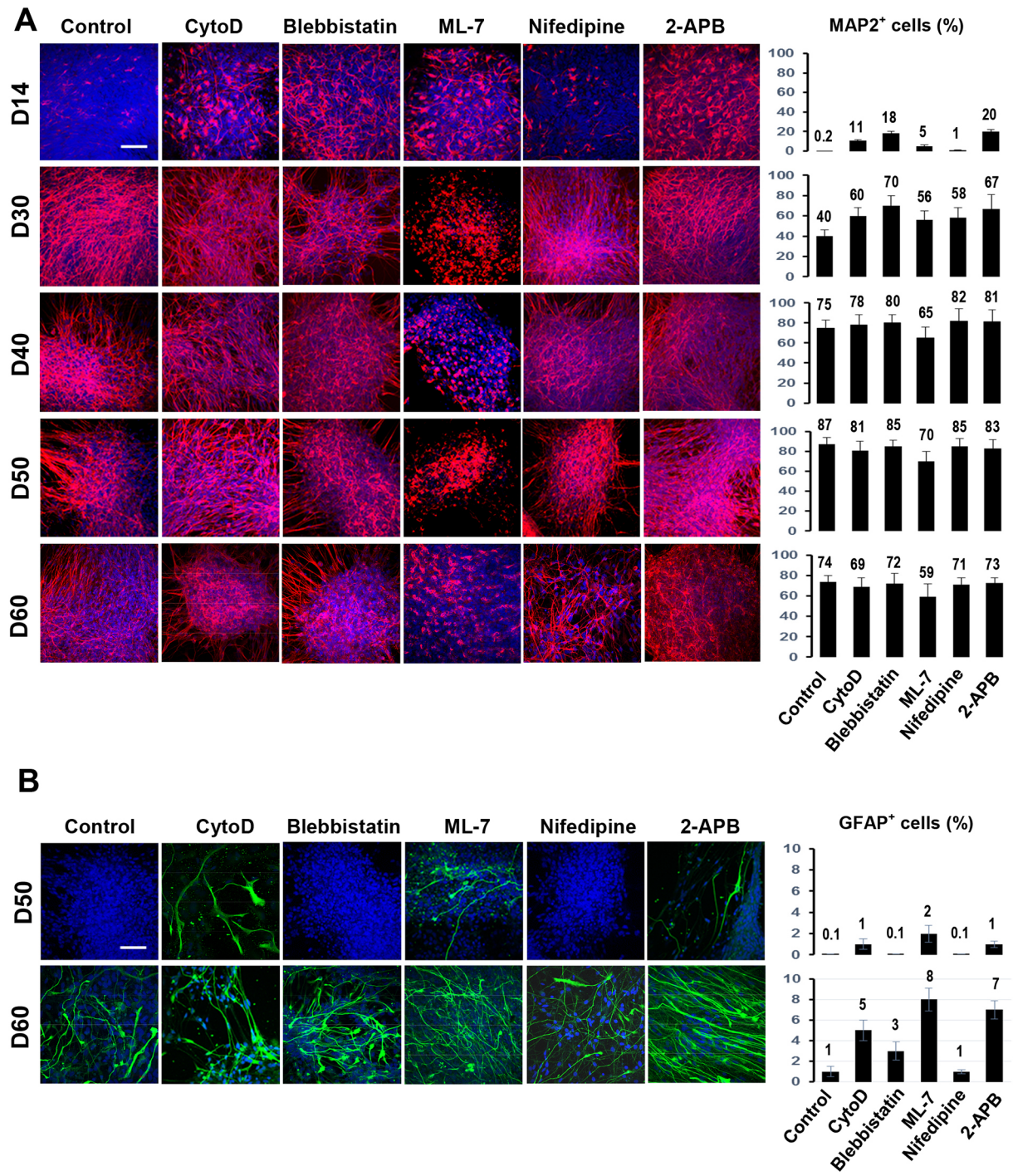

Fig. 8. Effects of inhibition of Ca^{2+}, actin and myosin II on neural fate decisions. Neural rosettes derived from human ESCs were treated continuously with several blockers from D11. The blockers used were: cytochalasin D (CytoD) (actin), blebbistatin (myosin II), ML-7 (myosin light chain kinase), nifedipine (Ca^{2+}) and 2-APB (Ca^{2+}). Cells were fixed on various days as indicated. (A) The generation of neurons from each sample was obtained by using immunocytochemical analysis; MAP2 is stained red and nuclei are stained blue with DAPI. The percentages of $MAP2^+$ neurons in each sample on different days of differentiation are shown on the right. (B) Astrocytes were detected from D50; GFAP is stained green and nuclei are stained blue with DAPI. The percentages of $GFAP^+$ astrocytes in each sample are shown on the right. Experiments were repeated twice. Data are mean±s.e.m. (*n*=2). Scale bars: 50 µm.

tight junctions, ZO-1 and occludin. Tight junctions and adherens junction complexes play crucial roles in epithelial cell polarization, enabling the conversion of primordial 'spot-like' adherens junction complexes to 'belt-like' adherens junctions by interacting with actin filaments (Irie et al., 2004; Vasioukhin et al., 2000). Ikenouchi et al. (2007) suggested that ZO-1 is directly involved in the establishment of two distinct junctional domains – belt-like adherens junctions and tight junctions – during epithelial polarization. Moreover, ZO-1 or ZO-2 is required for the activation of Rac1 during cell polarization, which acts upstream from the polarity protein components PARD3, PARD6 and aPKCλ/ζ (Mertens et al., 2005; Nishimura et al., 2005). Our results show that knockdown of ZO-1 derails the apical

Journal of Cell Science (2018) 131, jcs206896. doi:10.1242/jcs.206896

polarization of PARD3, β-catenin and tubulin, which leads to the eradication of cell elongation and lumen formation. Our finding is supported by a recent study in which kidney epithelia lacking ZO-1 were defective from the earliest phases of polarization and ZO-1 was necessary for lumen formation, which was regulated by cell-intrinsic signals via interactions between ZO-1 and occludin (Odenwald et al., 2017). Our results also indicate that lumen formation in neural rosettes is facilitated by apoptosis-mediated cavitation, which mirrors the findings observed in salivary glands (Andrew and Ewald, 2010; Teshima et al., 2016) and MDCK cysts (Martín-Belmonte et al., 2008).

Multicellular rosettes are one of the crucial shapes during morphogenesis in diverse organ systems and play an important role in brain development. It has been demonstrated that neural rosettes recapitulate the developmental steps of embryonic brains (Banda et al., 2015; Curchoe et al., 2012; Elkabetz et al., 2008; Grabiec et al., 2016; Hříbková et al., 2017; Paşca et al., 2015). The cytoarchitecture of neural rosettes provides regulatory micro-environments (or niches) to balance between NSC proliferation and differentiation. Some studies used a quantitative live imaging framework to characterize INM dynamics and show that those dynamics reflect the capability of NSCs in cell proliferation, suggesting the structure of neural rosettes hosts stem cell niches (Abranches et al., 2009; Ziv et al., 2015). Our previous study demonstrated that FGF2 signaling residing in the apical region of neural rosettes regulates rosette formation. The malformation of neural rosettes mediated by dysregulation of FGF2 signaling is in part attributed to the displacement of ZO-1 and the inhibition of FGF2 signaling, which leads to an increase in the numbers of cells exiting the cell cycle, a reduction in cell proliferation, and premature neurogenesis (Grabiec et al., 2016). In the current study, we further demonstrate that the dismantlement of neural rosettes mediated by the destruction of cytoskeletal elements promotes neurogenesis and astrogenesis prematurely, suggesting that an intact rosette structure is essential for orderly neural development.

In conclusion, this study shows that neural rosette formation consists of five types of cell movement, including intercalation, constriction, polarization, elongation and lumen formation. We also demonstrate that Ca^{2+} signaling plays a pivotal role in these five steps by regulating the actions of the cytoskeletal complexes, actin, myosin II and tubulin in intercalation, constriction and elongation. These actions, in turn, control the polarizing elements ZO-1, PARD3 and β-catenin in polarization and lumen formation during the course of neural rosette formation.

MATERIALS AND METHODS

Formation of human neural rosettes

Human ESCs (CCTL14; passage 25–40) were plated onto Matrigel-coated plates at 1000 cells/cm^2. Matrigel was purchased from BD Biosciences. The next day, cells were treated with 20 µM SB431542 (Tocris) in N2B27 medium for 2 days. The medium was changed every other day. Neural induction occurred on around D4. Neural stem cells then organized to form rosette structures. Neural rosettes appeared on D8–D9 (Grabiec et al., 2016). The experiments were designed to investigate how neural rosettes formed and determine what effects drugs had on rosette formation. Testing was carried out from D4 to D9. Drugs were tested individually using continuous cell exposure (treatment) starting at day 4 of differentiation; the exception was cyto D (cells treated for 5 h/day) and nocodazole (cells treated for 3 h/day) owing to toxicity. Control cells were treated with DMSO accordingly. Samples were collected and fixed at D5, D6, D7, D8 and D9. The drug treatments were: nocodazole (1 µM, Sigma), cyto D (1 µM, Invitrogen), ML-7 (10 µM, Sigma), blebbistatin (20 µM, Sigma), 2-APB (50 µM, Sigma) and nifedipine (20 µM, Sigma).

Effects of Ca^{2+} and cytoskeleton inhibitors on neural fate decisions

Human ESC-derived neural rosettes were harvested by manually cutting out, using pulled pipette tools, at D8 differentiation and transferred to dishes coated with fibronectin (Sigma) and Matrigel. The neural rosettes were continuously treated with the following inhibitors (except Cyto D) 3 days after re-plating: 2-APB (50 µM), blebbistatin (10 µM), cytochalasin D (1 µM), ML-7 (5 µM) and nifedipine (10 µM). Cells were treated with cytochalasin D for only 2 h and only on days with a medium change, owing to toxicity. Inhibitors were replenished every 3 days during medium changes. Samples were collected and fixed at various stages of differentiation (D14, D30, D40, D50 and D60). Cells were stained with MAP2 (a neuronal marker) and GFAP (an astrocyte marker) according to the procedures described previously (Lin et al., 2010; Matulka et al., 2013). Images were captured using a confocal microscope (LSM700, Carl Zeiss GmbH, Germany). Percentages of MAP2$^+$ and GFAP$^+$ cells in the whole cell population were estimated using a tissue scanner (TissueFaxs, Carl Zeiss, Germany).

HBSS treatment

Neural rosettes were harvested from D8 and placed onto Matrigel- and fibronectin-coated plates until they settled. To investigate the short-term effect of a Ca^{2+}-free environment on neural rosettes, neural rosettes transfected with the pEF1a-AcGFP1-N1 vector were placed in HBSS buffer (Invitrogen) for 30 min to 3 h and then HBSS was replaced with N2B27 medium. Changes in neural rosettes were recorded overnight using a time-lapse feature of a Zeiss confocal system. To investigate the destruction of neural rosettes under a Ca^{2+}-free environment, neural rosettes were treated with HBSS for 4 h, during which cell samples were collected and fixed at various time points (30 min, 1 h, 2 h and 4 h). Samples were stained with ZO-1 and β-catenin.

Time-lapse imaging

Investigation of dynamic neural rosettes was carried out using the time-lapse feature of a BioStation CT (Nikon Corporation, Japan). Harvested neural rosettes were filmed and image acquisition timing was set to one picture per 30 min. Images were processed using built-in software. The effects of HBSS and 2-APB on neural rosettes transfected with the pEF1a-AcGFP1-N1 vector were filmed at 1 image/5 min using a confocal microscope system (LSM 700, Carl Zeiss, Germany). The time-lapse movies and pictures were analyzed using Zen Blue and Black software (Carl Zeiss, Germany).

Involvement of apoptosis in lumen formation and neurogenesis

To investigate the role of apoptosis in lumen formation, neural stem cells were treated continuously with 10 µM, 20 µM or 40 µM z-VAD (Enzo Life Sciences), while control cells were treated with DMSO from D6. Media were changed every other day. Cell samples were fixed at D9 and stained with cleaved anti-caspase-3 and anti-ZO-1 antibodies. To investigate the relationship between the lumen and neurogenesis, neural stem cells were treated continuously with 40 µM Z-VAD from D6. Cell samples were fixed at D20 and stained with the neuronal marker MAP2.

Immunocytochemical analysis

ICC was performed as described previously (Lin et al., 2010; Matulka et al., 2013). In general, fixed cells were washed, permeabilized with 0.1% Triton X-100 in PBS for 1 hour at room temperature, and incubated with primary antibodies [from Sigma: mouse MAP2 (1:1000, M4403), rabbit β-catenin (1:1000, C2206), rabbit actin (1:300, A2066) and rabbit PARD3 (1:500, HPA030443); goat GFAP (Santa Cruz, 1:200, sc-6170); mouse ZO-1 (Invitrogen, 1:500, 339100); mouse tubulin (ExBio, 1:300, 11-250-M001); rabbit cleaved caspase-3 (Cell Signaling, 1:300, 9661S)] overnight at 4°C. The next day, cells were washed with PBS and incubated with DAPI (1:1500 in PBS) for 5 min. Next, the corresponding Alexa Fluor 488- or 594-conjugated secondary antibodies (Invitrogen, 1:500, A-21202, A-21203, A-21206, A-21207, A-11055) were added and incubated at room temperature for 1 hour. The stained cells were examined using a confocal microscope (LSM 700, Carl Zeiss, Germany).

Electron microscopy

To further characterize cell morphology, we examined the ultrastructure of neural rosettes using transmission electron microscopy (TEM). Human ESC-derived neural rosettes were harvested at D8 and seeded onto 4-well plates layered on a sheet of ACLAR Fluoropolymer Film (Electron Microscopy Sciences); these were then coated with Matrigel and fibronectin. Rosettes were maintained in N2B27 medium until D11, D13, D17, D20 and D24, and then the rosettes were fixed using 3% glutaraldehyde (Sigma-Aldrich) with 1% osmium tetroxide (Sigma-Aldrich) for 45 min at room temperature. Subsequently, they were washed three times for 10 min each, with 0.1 M cacodylate buffer and dehydrated with an increasing alcohol series (30%, 50%, 70%, 96% and 100%). After dehydration, the rosettes were embedded in LR white resin (Sigma-Aldrich) that was polymerized under UV light for 2 days at 4°C. Ultra-thin sections were prepared using an ultramicrotome (Leica EM UC6) and contrasted using 2% uranyl acetate and Reynolds' lead citrate. The sections were examined using a Morgagni 268D transmission electron microscope (FEI Company, Eindhoven, The Netherlands) equipped with a Veleta CCD Camera (Olympus, Münster, Germany).

The role of ZO-1 in neural rosette formation

The ZO-1 knockdown (KD) hESC (CCTL 14) line was generated using a ZO-1 shRNA vector (SHCLND-NM_175610, Sigma-Aldrich) and the mission PLKO.1-PURO vector (SHC001, Sigma-Aldrich) was used as a control, as described in our previous study (Grabiec et al., 2016). We used the ZO-1 KD hESC and control lines to investigate the effect of dysregulation of ZO-1 on neural rosette formation. ZO-1 mutant and control hESC lines were plated onto Matrigel-coated plates and were subjected to our neural differentiation paradigm described above. Cells samples were fixed at D5, D6, D7, D8 and D9 and stained for β-catenin, PARD3 and tubulin as described above.

Acknowledgements

We thank Dr M. Varecha for processing the 3D animation of Movies 1 and 2. We also thank Stephen J. Wadeley for proofreading our manuscript.

Competing interests

The authors declare no competing or financial interests.

Author contributions

Conceptualization: Y.-M.S.; Methodology: H.H., M.G., Y.-M.S.; Formal analysis: H.H., Y.-M.S.; Investigation: H.H., M.G., D.K., Y.-M.S.; Resources: I.S., Y.-M.S.; Data curation: Y.S.; Writing - original draft: Y.-M.S.; Writing - review & editing: H.H., M.G., I.S., Y.-M.S.; Visualization: Y.-M.S.; Supervision: Y.S.; Project administration: H.H., Y.-M.S.; Funding acquisition: Y.-M.S.

Funding

This study was supported by grants from the Czech Republic Ministry of Health (Ministerstvo zdravotnictví České republiky; 15-31063A), the Ministry of Education, Youth and Sport of the Czech Republic (Ministerstvo školství, mládeže a tělovýchovy České republiky; MSM0021622430 and CZ.1.07/2.3.00/ 20.0011) and the Grant Agency of Masaryk University (MUNI/A/0810/2016).

Supplementary information

Supplementary information available online at
http://jcs.biologists.org/lookup/doi/10.1242/jcs.206896.supplemental

References

Abranches, E., Silva, M., Pradier, L., Schulz, H., Hummel, O., Henrique, D. and Bekman, E. (2009). Neural differentiation of embryonic stem cells in vitro: a road map to neurogenesis in the embryo. *PLoS ONE* **4**, e6286.

Afonso, C. and Henrique, D. (2006). PAR3 acts as a molecular organizer to define the apical domain of chick neuroepithelial cells. *J. Cell Sci.* **119**, 4293-4304.

Andrew, D. J. and Ewald, A. J. (2010). Morphogenesis of epithelial tubes: insights into tube formation, elongation, and elaboration. *Dev. Biol.* **341**, 34-55.

Banda, E., McKinsey, A., Germain, N., Carter, J., Anderson, N. C. and Grabel, L. (2015). Cell polarity and neurogenesis in embryonic stem cell-derived neural rosettes. *Stem Cells Dev.* **24**, 1022-1033.

Blankenship, J. T., Backovic, S. T., Sanny, J. S. P., Weitz, O. and Zallen, J. A. (2006). Multicellular rosette formation links planar cell polarity to tissue morphogenesis. *Dev. Cell.* **11**, 459-470.

Bornens, M. and Azimzadeh, J. (2008). 'Origin and Evolution of the Centrosome'. Eukaryotic Membranes and Cytoskeleton. *Adv. Exp. Med. Biol.* **607**, 119-129.

Boroviak, T. and Rashbass, P. (2011). The apical polarity determinant Crumbs 2 is a novel regulator of ESC-derived neural progenitors. *Stem Cells* **29**, 193-205.

Bothwell, J. H. F., Kisielewska, J., Genner, M. J., McAinsh, M. R. and Brownlee, C. (2008). Ca2+ signals coordinate zygotic polarization and cell cycle progression in the brown alga *Fucus serratus*. *Development* **135**, 2173-2181.

Brennan, C., Mangoli, M. and Dyer, C. E. F. (2005). Ashworth R. Acetylcholine and calcium signaling regulates muscle fibre formation in the zebrafish embryo. *J. Cell Sci.* **118**, 5181-5190.

Cheng, A., Wang, S., Cai, J., Rao, M. S. and Mattson, M. P. (2003). Nitric oxide acts in a positive feedback loop with BDNF to regulate neural progenitor cell proliferation and differentiation in the mammalian brain. *Dev. Biol.* **258**, 319-333.

Collado-Hilly, M., Shirvani, H., Jaillard, D. and Mauger, J.-P. (2010). Differential redistribution of Ca2+-handling proteins during polarisation of MDCK cells: Effects on Ca2+ signalling. *Cell Calcium.* **48**, 215-224.

Colleoni, S., Galli, C., Giannelli, S. G., Armentero, M.-T., Blandini, F., Broccoli, V. and Lazzari, G. (2010). Long-term culture and differentiation of CNS precursors derived from anterior human neural rosettes following exposure to ventralizing factors. *Exp. Cell Res.* **316**, 1148-1158.

Colosetti, P., Tunwell, R. E., Cruttwell, C., Arsanto, J.-P., Mauger, J. P. and Cassio, D. (2003). The type 3 inositol 1,4,5-trisphosphate receptor is concentrated at the tight junction level in polarized MDCK cells. *J. Cell Sci.* **116**, 2791-2803.

Cruttwell, C., Bernard, J., Hilly, M., Nicolas, V., Tunwell, R. E. and Mauger, J.-P. (2005). Dynamics of the Ins(1,4,5)P3 receptor during polarization of MDCK cells. *Biol. Cell.* **97**, 699-707.

Curchoe, C. L., Russo, J. and Terskikh, A. V. (2012). hESC derived neuro-epithelial rosettes recapitulate early mammalian neurulation events; an *in vitro* model. *Stem Cell Res.* **8**, 239-246.

Dupin, I., Camand, E. and Etienne-Manneville, S. (2009). Classical cadherins control nucleus and centrosome position and cell polarity. *J. Cell Biol.* **185**, 779-786.

Elkabetz, Y., Panagiotakos, G., Al Shamy, G., Socci, N. D., Tabar, V. and Studer, L. (2008). Human ES cell-derived neural rosettes reveal a functionally distinct early neural stem cell stage. *Genes Dev.* **22**, 152-165.

Eom, D. S., Amarnath, S., Fogel, J. L. and Agarwala, S. (2011). Bone morphogenetic proteins regulate neural tube closure by interacting with the apicobasal polarity pathway. *Development* **138**, 3179-3188.

Evans, J. H. and Falke, J. J. (2007). Ca2+ influx is an essential component of the positive-feedback loop that maintains leading-edge structure and activity in macrophages. *Proc. Natl. Acad. Sci. USA* **104**, 16176-16181.

Falk, A., Heine, V. H., Harwood, A. J., Sullivan, P. F., Peitz, M., Brüstle, O., Shen, S., Sun, Y.-M., Glover, J. C., Posthuma, D. et al. (2016). Modeling psychiatric disorders: from genomic findings to cellular phenotypes. *Mol. Psychiatry.* **21**, 1167-1179.

Gaiano, N. and Fishell, G. (2002). The role of notch in promoting glial and neural stem cell fates. *Annu. Rev. Neurosci.* **25**, 471-490.

Gilbert, S. F. (2010). *Developmental Biology*, 9th edn, Chapter 8-9, pp. 300-372. Sunderland, Massachusetts USA: SinauerAssociates, Inc.

Glotfelty, L. G., Zahs, A., Iancu, C., Shen, L. and Hecht, G. A. (2014). Microtubules are required for efficient epithelial tight junction homeostasis and restoration. *Am. J. Physiol. Cell Physiol.* **307**, C245-C254.

Gompel, N., Cubedo, N., Thisse, C., Thisse, B., Dambly-Chaudière, C. and Ghysen, A. (2001). Pattern formation in the lateral line of zebrafish. *Mech. Dev.* **105**, 69-77.

Grabiec, M., Hříbková, H., Vařecha, M., Střítecká, D., Hampl, A., Dvořák, P. and Sun, Y.-M. (2016). Stage-specific roles of FGF2 signaling in human neural development. *Stem Cell Res.* **17**, 330-341.

Hable, W. E. and Hart, P. E. (2010). Signaling mechanisms in the establishment of plant and fucoid algal polarity. *Mol. Reprod. Dev.* **77**, 751-758.

Haigo, S. L., Hildebrand, J. D., Harland, R. M. and Wallingford, J. B. (2003). Shroom induces apical constriction and is required for hingepoint formation during neural tube closure. *Curr. Biol.* **13**, 2125-2137.

Harding, M. J., McGraw, H. F. and Nechiporuk, A. (2014). The roles and regulation of multicellular rosette structures during morphogenesis. *Development* **141**, 2549-2558.

Himschoot, E., Beeckman, T., Friml, J. and Vanneste, S. (2015). Calcium is an organizer of cell polarity in plants. *Biochim. Biophys. Acta.* **1853**, 2168-2172.

Hoffman, L., Farley, M. M. and Waxham, M. N. (2013). "Calcium-calmodulin-dependent protein kinase II isoforms differentially impact the dynamics and structure of the actin cytoskeleton. *Biochemistry* **52**, 1198-1207.

Hříbková, H., Zelinková, J. and Sun, Y.-M. (2017). Progress in human pluripotent stem cell-based modeling systems for neurological diseases. *Neurogenesis* **4**, Iss: 1, e1324258 (p1-6).

Huang, Z.-H., Wang, Y., Su, Z.-D., Geng, J.-G., Chen, Y.-Z., Yuan, X.-B. and He, C. (2011). Slit-2 repels the migration of olfactory ensheathing cells by triggering Ca 2+-dependent cofilin activation and RhoA inhibition. *J. Cell Sci.* **124**, 186-197.

Huang, Y.-W., Chang, S.-J., Harn, H., Huang, H.-T., Lin, H.-H., Shen, M.-R., Tang, M.-J. and Chiu, W.-T. (2015). Mechanosensitive store-operated calcium entry regulates the formation of cell polarity. *J. Cell. Physiol.* **230**, 2086-2097.
Ikenouchi, J., Umeda, K., Tsukita, S., Furuse, M. and Tsukita, S. (2007). Requirement of ZO-1 for the formation of belt-like adherens junctions during epithelial cell polarization. *J. Cell Biol.* **176**, 779-786.
Irie, K., Shimizu, K., Sakisaka, T., Ikeda, W. and Takai, Y. (2004). Roles and modes of action of nectins in cell-cell adhesion. *Semin. Cell Dev. Biol.* **15**, 643-656.
Lancaster, M. A., Renner, M., Martin, C.-A., Wenzel, D., Bicknell, L. S., Hurles, M. E., Homfray, T., Penninger, J. M., Jackson, A. P. and Knoblich, J. A. (2013). Cerebral organoids model human brain development and microcephaly. *Nature* **501**, 373-379.
Larsson, C. (2006). Protein kinase C and the regulation of the actin cytoskeleton. *Cell. Signal.* **18**, 276-284.
Lienkamp, S. S., Liu, K., Karner, C. M., Carroll, T. J., Ronneberger, O., Wallingford, J. B. and Walz, G. (2012). Vertebrate kidney tubules elongate using a planar cell polarity-dependent, rosette-based mechanism of convergent extension. *Nat. Genet.* **44**, 1382-1387.
Lin, H.-H., Bell, E., Uwongoho, D., Perfect, L. W., Noristani, H., Bates, T. J., Snetkov, V., Price, J. and Sun, Y.-M. (2010). Neuronatin promotes neural lineage in ESCs via Ca^{2+} signaling. *Stem Cells* **28**, 1950-1960.
Main, H., Radenkovic, J., Jin, S.-B., Lendahl, U. and Andersson, E. R. (2013). Notch signaling maintains neural rosette polarity. *PLoS ONE* **8**, e62959.
Martín-Belmonte, F., Yu, W., Rodríguez-Fraticelli, A. E., Ewald, A. J., Werb, Z., Alonso, M. A. and Mostov, K. (2008). Cell-polarity dynamics controls the mechanism of lumen formation in epithelial morphogenesis. *Curr. Biol.* **18**, 507-513.
Matulka, K., Lin, H.-H., Hříbková, H., Uwanogho, D., Dvořák, P. and Sun, Y.-M. (2013). PTP1B is an effector of activin signaling and regulates neural specification of embryonic stem cells. *Cell Stem Cell* **13**, 706-719.
Mertens, A. E. E., Rygiel, T. P., Olivo, C., van der Kammen, R. and Collard, J. G. (2005). The Rac activator Tiam1 controls tight junction biogenesis in keratinocytes through binding to and activation of the Par polarity complex. *J. Cell Biol.* **170**, 1029-1037.
Mirzadeh, Z., Merkle, F. T., Soriano-Navarro, M., Garcia-Verdugo, J. M. and Alvarez-Buylla, A. (2008). Neural stem cells confer unique pinwheel architecture to the ventricular surface in neurogenic regions of the adult brain. *Cell Stem Cell.* **3**, 265-278.
Nishimura, T. and Takeichi, M. (2008). Shroom3-mediated recruitment of Rho kinases to the apical cell junctions regulates epithelial and neuroepithelial planar remodeling. *Development* **135**, 1493-1502.
Nishimura, T., Yamaguchi, T., Kato, K., Yoshizawa, M., Nabeshima, Y., Ohno, S., Hoshino, M. and Kaibuchi, K. (2005). PAR-6-PAR-3 mediates Cdc42-induced Rac activation through the Rac GEFs STEF/Tiam1. *Nat. Cell Biol.* **7**, 270-277.
Odenwald, M. A., Choi, W., Buckley, A., Shashikanth, N., Joseph, N. E., Wang, Y., Warren, M. H., Buschmann, M. M., Pavlyuk, R., Hildebrand, J. et al. (2017). ZO-1 interactions with F-actin and occludin direct epithelial polarization and single lumen specification in 3D culture. *J. Cell Sci.* **130**, 243-259.
Oteiza, P., Köppen, M., Krieg, M., Pulgar, E., Farias, C., Melo, C., Preibisch, S., Müller, D., Tada, M., Hartel, S. et al. (2010). Planar cell polarity signalling regulates cell adhesion properties in progenitors of the zebrafish laterality organ. *Development* **137**, 3459-3468.
Paşca, A. M., Sloan, S. A., Clarke, L. E., Tian, Y., Makinson, C. D., Huber, N., Kim, C. H., Park, J.-Y., O'Rourke, N. A., Nguyen, K. D. et al. (2015). Functional cortical neurons and astrocytes from human pluripotent stem cells in 3D culture. *Nat. Methods* **12**, 671-678.
Perrier, A. L., Tabar, V., Barberi, T., Rubio, M. E., Bruses, J., Topf, N., Harrison, N. L. and Studer, L. (2004). Derivation of midbrain dopamine neurons from human embryonic stem cells. *Proc. Natl. Acad. Sci. USA* **101**, 12543-12548.
Petersen, O. H. and Tepikin, A. V. (2008). Polarized calcium signaling in exocrine gland cells. *Annu. Rev. Physiol.* **70**, 273-299.
Sackmann, E. (2015). How actin/myosin crosstalks guide the adhesion, locomotion and polarization of cells. *Biochim. Biophys. Acta.* **1853**, 3132-3142.
Shen, L. and Turner, J. R. (2005). Actin depolymerization disrupts tight junctions via caveolae-mediated endocytosis. *Mol. Biol. Cell.* **16**, 3919-3936.
Shi, Y., Kirwan, P., Smith, J., Robinson, H. P. C. and Livesey, F. J. (2012). Human cerebral cortex development from pluripotent stem cells to functional excitatory synapses. *Nat. Neurosci.* **15**, 477-486.
Shindo, A., Hara, Y., Yamamoto, T. S., Ohkura, M., Nakai, J. and Ueno, N. (2010). Tissue-tissue interaction-triggered calcium elevation is required for cell polarization during Xenopus gastrulation. *PLoS ONE* **5**, e8897.
Sun, Y. -M., Cooper, M., Finch, S., Lin, H. -H., Chen, Z.-F., Williams, B. P. and Buckley, N. J. (2008). REST- mediated regulation of extracellular matrix is crucial for neural development. *PLoS ONE* **3**, e3656.
Teshima, T. H. N., Wells, K. L., Lourenço, S. V. and Tucker, A. S. (2016). Apoptosis in early salivary gland duct morphogenesis and lumen formation. *J. Dent. Res.* **95**, 277-283.
Trichas, G., Smith, A. M., White, N., Wilkins, V., Watanabe, T., Moore, A., Joyce, B., Sugnaseelan, J., Rodriguez, T. A., Kay, D. et al. (2012). Multi-cellular rosettes in the mouse visceral endoderm facilitate the ordered migration of anterior visceral endoderm cells. *PLoS Biol.* **10**, e1001256.
Tsai, F.-C. and Meyer, T. (2012). Ca2+ pulses control local cycles of lamellipodia retraction and adhesion along the front of migrating cells. *Curr. Biol.* **22**, 837-842.
Vasioukhin, V., Bauer, C., Yin, M. and Fuchs, E. (2000). Directed actin polymerization is the driving force for epithelial cell-cell adhesion. *Cell* **100**, 209-219.
Villasenor, A., Chong, D. C., Henkemeyer, M. and Cleaver, O. (2010). Epithelial dynamics of pancreatic branching morphogenesis. *Development* **137**, 4295-4305.
Wallingford, J. B., Ewald, A. J., Harland, R. M. and Fraser, S. E. (2001). Calcium signaling during convergent extension in Xenopus. *Curr. Biol.* **11**, 652-661.
Webb, S. E. and Miller, A. L. (2003). Imaging intercellular calcium waves during late epiboly in intact zebrafish embryos. *Zygote* **11**, 175-182.
Webb, S. E. and Miller, A. L. (2006). Ca2+ signaling during vertebrate somitogenesis. *Acta Pharmacol. Sin.* **27**, 781-790.
Wilson, P. G. and Stice, S. S. (2006). Development and differentiation of neural rosettes derived from human embryonic stem cells. *Stem Cell Rev.* **2**, 67-77.
Yanagawa, N., Sakabe, M., Sakata, H., Yamagishi, T. and Nakajima, Y. (2011). Nodal signal is required for morphogenetic movements of epiblast layer in the pre-streak chick blastoderm. *Dev. Growth Differ.* **53**, 366-377.
Zhang, S.-C., Wernig, M., Duncan, I. D., Brüstle, O. and Thomson, J. A. (2001). In vitro differentiation of transplantable neural precursors from human embryonic stem cells. *Nat. Biotechnol.* **19**, 1129-1133.
Ziv, O., Zaritsky, A., Yaffe, Y., Mutukula, N., Edri, R. and Elkabetz, Y. (2015). Quantitative live imaging of human embryonic stem cell derived neural rosettes reveals structure-function dynamics coupled to cortical development. *PLoS Comput. Biol.* **11**, e1004453.

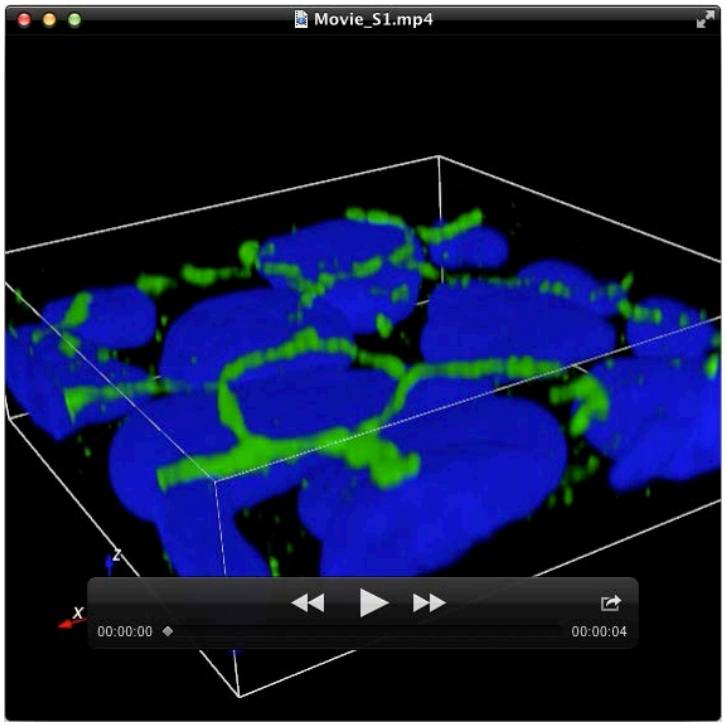

Movie S1:

The location of the tight junction protein, ZO-1, in neural stem cells derived from human embryonic stem cells.

Human embryonic stem cells were driven towards neural lineage, during which process neural stem cells appeared at 4-day differentiation and neural rosettes formed at 9 days of differentiation. Cells were fixed and stained with ZO-1 antibody (green) and DAPI (blue) at 5-day differentiation. The 3-D animation was generated from one of the Z-stack images taken from 5-day differentiation using Black Zen software (Zeiss). ZO-1 can be clearly seen locating at the tight junction in a group of neural stem cells. The directions of the X,Y, and Z axes are indicated on the bottom left.

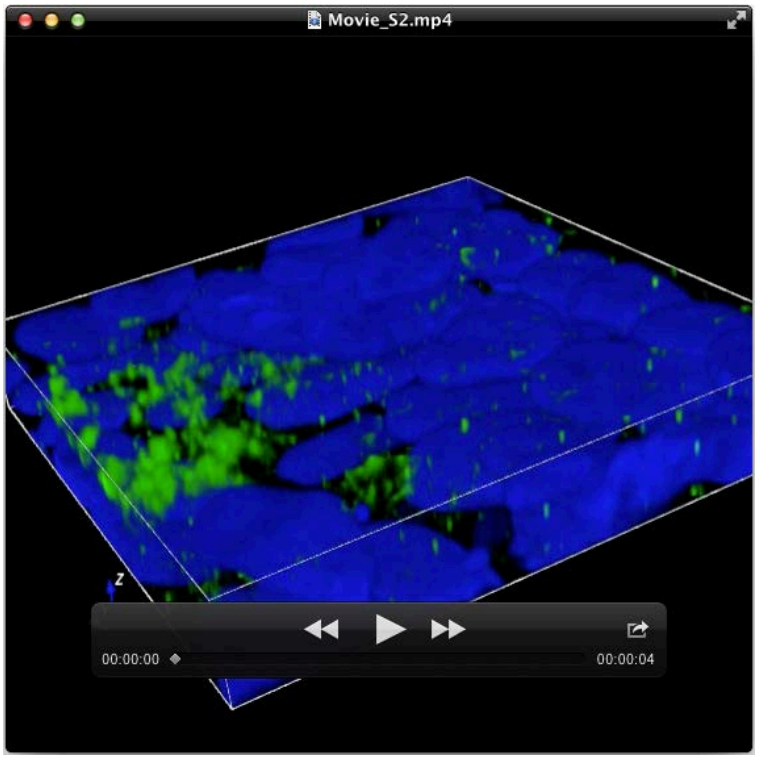

Movie S2:

The polarization of the tight junction protein, ZO-1, during neural rosette formation.

Human embryonic stem cells were driven towards neural lineage, during which process neural stem cells appeared at 4-day differentiation and neural rosettes formed at 9 days of differentiation. Cells were fixed and stained with ZO-1 antibody (green) and DAPI (blue) at 7-day differentiation, when neural rosettes were starting to take shape. The 3-D animation was generated from one of the Z-stack images taken from 7 days of differentiation using Black Zen software (Zeiss). The movie shows that the location of ZO-1 in the tight junction (see Movie S1) is breaking down and the protein relocates to the apical region of neural rosettes. The directions of the X,Y, and Z axes are indicated on the bottom left.

Movie S3:

The dynamic nature of neural rosette lumens.

Human neural rosettes were harvested at 10-day differentiation and were transferred to a new Matrigel and fibronectin-coated plate. Spread-out neural rosettes were subjected to time-lapse imaging using BioStation CT (Nikon Corporation, Japan). Image acquisition timing was set to every 30 min per picture for 3 days. The movie presented here was a part of a full-length film. The movie shows that the lumens of neural rosettes are constantly reshaping or re-structuring when rosettes are growing and thickening, indicating the dynamic nature of the lumens.

Journal of Cell Science • Supplementary information

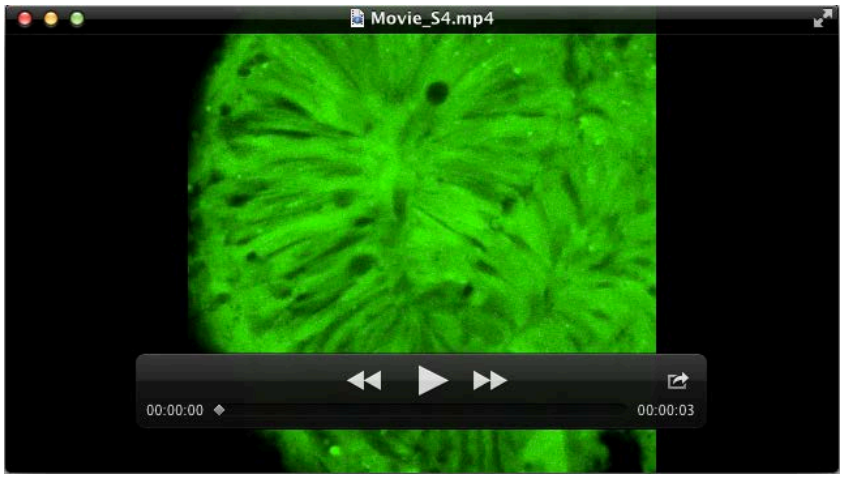

Movie S4:

The effect of calcium-free environment on neural rosette maintenance.

Neural rosettes were derived from human embryonic stem cells stably transfected with the pEF1a-AcGFP1-N1 vector. Time lapse imaging of a neural rosette responding to calcium-free HBSS buffer was filmed before HBSS treatment for 10 min in N2B27 medium, then changed to HBSS buffer for 3 hr, and in N2B27 medium after replacing HBSS buffer overnight. The movie was extracted from a full-length film, which was recorded at 1 picture/5 min using the confocal microscope system (LSM 700, Carl Zeiss GmbH, Germany). The movie depicts the structure of the neural rosette is undergoing dismantling in HBSS buffer, but restructuring and forming smaller neural rosettes in N2B27 medium overnight after lifting HBSS buffer, suggesting the effect of the absence of calcium in neural rosette maintenance is temporary if rescued in time (i.e. reinstalling the environment in N2B27 medium).

Journal of Cell Science • Supplementary information

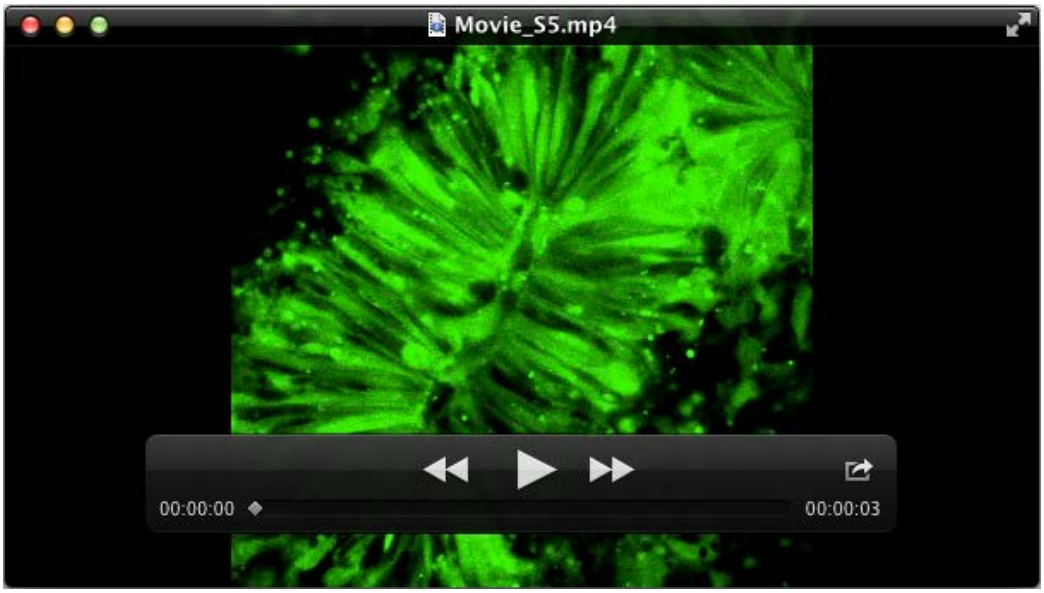

Movie S5:

The effect of 2-APB (an IP3 receptor blocker) on neural rosette maintenance.

Neural rosettes were derived from human embryonic stem cells stably transfected with the pEF1a-AcGFP1-N1 vector. Time lapse imaging of a neural rosette responding to 50 µM 2-Aminoethoxydiphenyl borate *(*2-APB) was filmed before treatment for 10 min in N2B27 medium, under 2-APB treatment for 3 hr, and in N2B27 medium after washing off 2-APB overnight. The movie was extracted from a full-length film, which was recorded at 1 picture/5 min using the confocal microscope system (LSM 700, Carl Zeiss GmbH, Germany). The movie depicts the partial dismantlement of a neural rosette under 2-APB treatment for 3 hr. However, the destructed neural rosette failed to form new neural rosettes in N2B27 medium overnight after lifting 2-APB treatment.

Journal of Cell Science • Supplementary information